Available online at www.sciencedirect.com

ScienceDirect

journal homepage: www.jfda-online.com

Original Article

Proanthocyanidins from the stem bark of *Rhus tripartita* ameliorate methylgloxal-induced endothelial cell apoptosis

Ali S. Alqahtani [a,b,**], *Wael M. Abdel-Mageed* [a,c], *Abdelaaty A. Shahat* [a,b,d,*], *Mohammad K. Parvez* [a], *Mohammed S. Al-Dosari* [a], *Ajamaluddin Malik* [e], *Maged S. Abdel-Kader* [f], *Mansour S. Alsaid* [a]

[a] *Department of Pharmacognosy, College of Pharmacy, King Saud University, P.O. Box 2457, Riyadh 11451, Saudi Arabia*

[b] *Medicinal Aromatic & Poisonous Plants Research Centre, College of Pharmacy, King Saud University, P.O. Box 2457, Riyadh 11451, Saudi Arabia*

[c] *Pharmacognosy Department, Faculty of Pharmacy, Assiut University, Assiut 71526, Egypt*

[d] *Phytochemistry Department, National Research Centre, 33 El Bohouth St. (former El Tahrir St.), 12622, Dokki, Giza, Egypt*

[e] *Protein Research Chair, Department of Biochemistry, College of Sciences, King Saud University, Riyadh 11451, Saudi Arabia*

[f] *Department of Pharmacognosy, Sattam Bin Abdulaziz University, College of Pharmacy, 11942, Al-kharj, Saudi Arabia*

ARTICLE INFO

Article history:
Received 8 December 2018
Received in revised form
17 January 2019
Accepted 11 February 2019
Available online 17 March 2019

Keywords:
Rhus tripartita
Proanthocyanidin
Oxidative stress
Endothelial dysfunction
Cardiovascular complications

ABSTRACT

In traditional Arabian medicine, the *Rhus tripartita* plant (family Anacardiaceae) has been used to treat inflammatory conditions. Although *Rhus* extracts have been reported for their cardioprotective effects, information regarding their active principle compounds remains insufficient. The present investigation was aimed at determining the antioxidant chemical constituents of the methanolic extract of *R. tripartita* stem bark and evaluating their ability to ameliorate methylglyoxal-induced endothelial cell apoptosis. Ten flavonoid compounds (**1**–**10**) were isolated and identified using DPPH radical scavenging bioassay-guided chromatographic separation. A new proanthocyanidin (rhuspartin) (**1**) was isolated and identified as 3,5,13,14-flavantetrol-(4β→8)-catechin, using extensive spectroscopic data and high resolution-mass spectrometry. Among the compounds (**1**, **5**, **7**–**10**) tested for toxicity toward cultured endothelial cells (HUVECs), the non-cytotoxic compounds **1** and **7** evinced cytoprotective potential that reversed the methylglyoxal-induced apoptosis (by 62% and 64%, respectively) through downregulation of caspase 3/7.

* *Corresponding author*. Department of Pharmacognosy, College of Pharmacy, King Saud University, P.O. Box 2457, Riyadh 11451, Saudi Arabia.

** *Corresponding author*. Department of Pharmacognosy, College of Pharmacy, King Saud University, P.O. Box 2457, Riyadh 11451, Saudi Arabia.

E-mail addresses: alalqahtani@ksu.edu.sa (A.S. Alqahtani), ashahat@ksu.edu.sa (A.A. Shahat).

https://doi.org/10.1016/j.jfda.2019.02.002

1. Introduction

The family Anacardiaceae, which consists of 73 genera and approximately 600 species [1,2], is comprised mainly of trees, shrubs, and/or woody vines. The majority of these belong to the genus *Rhus* [3,4], including over 250 species that bear the common name sumac [5]. It is widely distributed in the tropics, subtropics, and various global temperate zones and is known to be rich in flavonoids, bioflavonoids, and proanthocyanidins [6–10]. In particular, *Rhus tripartita* (Ucria) Grande is distributed primarily in North Africa and in northeastern part of Saudi Arabia [5]. In Arabian traditional medicine, this plant has been used for the treatment of cardiovascular and gastrointestinal disorders along with inflammatory conditions [5,11]; its other reported biological activities also include antioxidant, antidiarrheal, and antiulcer effects [12].

Methylglyoxal (MGO), a highly reactive dicarbonyl compound, is generated endogenously as well as in several foodstuffs and beverages during processing, cooking, or storage as a by-product of glycolysis [13,14]. High level of plasma MGO is associated with type 2 diabetes mellitus and considered as a causative factor in atherosclerosis and macrovascular diseases [15,16]. Notably, in cultured endothelial cells (ECs), MGO rapidly causes a hyperglycemic state that damages ECs function and becomes a prominent factor in most diabetic complications [17,18]. Furthermore, ECs play an important role in modulating vascular function and homeostasis; thus, their dysfunction as result of inflammation and apoptosis can be an initiating event in atherogenesis [19].

In our previous work, we demonstrated the therapeutic nature of *R. tripartita* stem bark including its cardiovascular, antioxidant, and anti-inflammatory effects [5,8]. The aim of the present study was to isolate and identify the antioxidant compounds, in particular those of phenolic nature, from the stem bark of *R. tripartita*. In addition, we assessed their activity toward reversing the endothelial apoptosis mediated by MGO to highlight the potential use of this plant as a source of safe and effective drugs against diabetic cardiovascular complications.

2. Materials and methods

2.1. General methods

Optical rotations were measured on a Perkin–Elmer Model 343 polarimeter (Waltham, MA, USA). CD spectra were recorded on a Jasco J-815 spectrophotometer in 1-cm cuvettes at room temperature. Nuclear magnetic resonance (NMR) spectra were recorded in deuterated dimethylsulfoxide (DMSO-d_6) on an UltraShield Plus system (Bruker Biospin GmbH, Rheinstetten, Germany) operating at 700 MHz for ^{1}H and at 175 MHz for ^{13}C. HPLC was carried out using a Phenomenex Jupiter Proteo column (Jupiter Proteo 90 Å, 250 × 10 mm, 4 μm; Torrance, CA, USA) on a Shimadzu HPLC-LC-20 AD series binary gradient pump and a Shimadzu SPD-M20A detector (Tokyo, Japan). Column chromatography (CC) was carried out on Sephadex LH-20 (Pharmacia, Uppsala, Sweden) using ethanol as the eluent.

2.2. Plant material

R. tripartita stem bark was collected from Hail in the northwestern region of Saudi Arabia in April 2013. The plant was identified and authenticated by an expert taxonomist at the Herbarium Unit, College of Pharmacy, King Saud University. The voucher specimen has been deposited (SY 202/2013) at the herbarium of the Faculty of Pharmacy, King Saud University, Riyadh, Saudi Arabia.

2.3. Extraction and isolation

Using 4000 ml of 80% aqueous methanol, 1100 g of air-dried powdered stem barks was extracted by maceration three times. The alcoholic extract was filtered and concentrated under reduced pressure at 40 °C to yield a dry extract of 231 g (21%). Part of the dry extract (100 g) was partitioned in 400 ml of distilled water and subjected successively to solvent fractionation with dichloromethane (CH_2Cl_2), ethyl acetate (EtOAc), and *n*-butanol (*n*-BuOH) (3 × 400 ml) until complete exhaustion in each fractionation step to yield a dichloromethane fraction (RTSM1) (7.3 g), ethyl acetate (RTSM2) (20 g), *n*-butanol (RTSM3) (8.7 g), and an aqueous fraction (RTSM4) (13.8 g). The EtOAc fraction (RTSM2) was subjected to gel filtration chromatography by using a Sephadex LH-20 column (Pharmacia) (90 × 4 cm) and EtOH as the mobile phase. The fractions (50 ml each) were collected and examined by thin-layer chromatography (TLC; Silica gel 60 F254 plate, Merck, Kenilworth, NJ, USA) using EtOAc-HOAc-HCOOH-H_2O (30/0.8/1.2/8) as the solvent system. The TLC plate was examined under UV (254 and 366 nm) before and after spraying with vanillin H_2SO_4 (reagent A) and Neu's spray reagent (reagent B). A total of 86 fractions were collected, and similar fractions were combined to yield seven groups: RTSM2-I, fr. 1–15; RTSM2-II, fr. 16–20; RTSM2-III, fr. 21–35; RTSM2-IV, fr. 36–45; RTSM2-V, fr. 46–60; RTSM2-VI, fr. 61–74; and RTSM2-VII, fr. 75–86. The sub-fractions was subjected to reversed-phase HPLC (Jupiter Proteo 90 Å, 250 × 10 mm, 4 μm) using a 5–70% CH_3CN–H_2O gradient over 40 min, and the following compounds were obtained: (**2**), 16.1 mg yellow amorphous powder; (**4**), 7.9 mg yellow amorphous powder, and (**5**), 11.6 mg yellow amorphous powder from RTSM2-II; (**3**) and (**6**), 10.2 and 3.8 mg yellow amorphous powders, respectively, from RTSM2-III; (**7**) and (**1**), 14.1 and 11.3 mg yellow amorphous powders, respectively, from RTSM2-IV; (**8**), (**9**) and (**10**), 9.1, 12.6 and 5.5 mg yellow amorphous powders, respectively, from RTSM2-V.

2.4. 1,1-Diphenyl-2-picrylhydrazyl (DPPH) radical-scavenging assay

The radical-scavenging activity of the isolated compounds against DPPH* was assessed with a rapid TLC screening method using 0.2% DPPH in MeOH. At 30 min after spraying, the active compounds appeared as yellow spots against a purple background [20,21].

2.5. Cell culture and compounds preparation

Human umbilical vein endothelial cells (HUVEC 16549) were maintained in Dulbecco's modified Eagle medium-GlutaMax (DMEM-GlutaMax) medium (Gibco, Gaithersburg, MD, USA), supplemented with 10% bovine serum (Gibco) and 1 × penicillin-streptomycin mix (Invitrogen, Carlsbad, CA, USA) at 37 °C with 5% CO_2 in a humid chamber. Stocks of compounds (**1**, **5**, **7**–**10**; 1 mg, each) were prepared by first dissolving in 50 μl DMSO (Sigma, Munich, Germany) and then in complete medium (1 mg/ml; DMSO <0.1%, final), followed by reconstitution in six working concentration (25, 12.5, 6.25, 3.12 and 1.56 μg/ml) in complete medium. The DMSO (<0.1%) acted as an untreated or negative control. The standard pro-apoptotic agent MGO [22] and anti-apoptotic drug aminoguanidine (AG) [23] were also prepared in DMSO and culture medium.

2.6. Cytotoxicity assay

The cytotoxic effect, if any, of compounds (**1**, **5**, **7**–**10**) was tested on HUVECs using the cell proliferation assay (TACS cell proliferation MTT assay Cell Proliferation Assay Kit, Trevigen, Gaithersbutg, MD, USA). Briefly, HUVECs (0.5 × 10^5/well) were seeded in a 96-well flat-bottom plate (Becton–Dickinson Labware, Bedford, MA, USA) and incubated overnight. The cells were treated with the different doses (in triplicate) of the test compounds, including untreated (DMSO) and positive (MGO) controls. At day 3 post-treatment, cells were treated with MTT reagent (10 μl/well) and incubated at room-temperature for 4 h in the dark. Immediately upon the appearance of purple color, detergent solution (100 μl/well) was added and the cells were further incubated for 1.5 h at 37 °C. The optical density (OD; λ = 570) was measured (Microplate reader ELx800; BioTek, Winooski, VT, USA). Non-linear regression analysis was performed (Excel 2010; Microsoft Corp., Redmond, WA, USA) to determine the cell proliferation fraction using the following equation:

$$\text{Cell proliferation fraction} = ODs - ODb / ODc - ODb$$

where ODs, ODb, and ODc are the absorbance of sample, blank, and negative control, respectively. Data were subjected to non-linear regression analysis (Excel) and presented as % cell survival in relation to the untreated control.

2.7. Anti-apoptotic/cytoprotective assay

The two non-cytotoxic compounds **1** and **7** were further tested for their cytoprotective/anti-apoptotic potential on HUVECs. In brief, HUVECs (0.5 × 10^5/well) were seeded in a 96-well flat-bottom plate (Becton–Dickinson Labware) and incubated overnight. The pro-apoptotic agent MGO (0.5 mM) was added to the cells followed by co-treatment with different doses (25, 12.5, 6.25 and 3.12 μg/ml) of **1** and **7** as well as the standard anti-apoptotic drug AG (0.05 mM) in triplicate. At day 3 post-incubation, MTT assay was performed as in section 2.6 and OD were measured. Data were subjected to non-linear regression analysis and presented as % increase in cell proliferation/survival in relation to the standard control.

2.8. Apoptotic signaling (caspase-3/7) assay

To assess *in vitro* caspase-3/7 activation, HUVECs (0.5 × 10^5/well) were treated with the anti-apoptotic compounds **1** and **7** (25 μg/ml, each), AG (0.05 mM), and MGO (0.5 mM), and were assayed on day 3 (Apo-ONE-cas3/7 Assay Kit; Promega, Madison, WI, USA) as per the supplied manual. Briefly, caspase-3/7 reagent was added (100 μl/well) and cells were incubated in the dark at room temperature for 5 h. The OD was measured, and data were subjected to non-linear regression analysis and presented as % inhibition of caspase-3/7 activity in relation to the standard control.

3. Results and discussion

3.1. Identification of isolated compound

A radical-scavenging guided phytochemical study on the stem bark of *R. tripartita* led to the isolation and identification of 10 flavonoids (Fig. 1). The structures of these compounds were elucidated by extensive 1D and 2D NMR analyses, accurate mass measurements, and comparison with reported data. The flavonoids were identified as catechin (**2**) [24], gallocatechin (**3**) [24], taxifolin (**4**) [25], epicatechin (**5**) [24], epigallocatechin (**6**) [24], epicatechin-3-*O*-rhamnoside (**7**) [26], mesuaferrone-A (**8**) [27], myricetin-3-*O*-glucopyranoside (**9**) [28], and 2″,3″-dihydrohinokiflavone (**10**) [29]. All physical and spectral data of these compounds were in agreement with the respective published data.

Rhuspartin (**1**) was obtained as a yellow amorphous solid ($[\alpha]^{25}_D$ 144.7° (*c* 0.3, MeOH)). High-resolution electrospray ionization mass spectrometry (HRESIMS) showed a pseudo-molecular ion peak at *m/z* 561.1400 $[M-H]^-$ (calcd 561.1402) consistent with a molecular weight of 562 amu. The molecular formula was established as $C_{30}H_{26}O_{11}$, implying 18 degrees of unsaturation. The UV spectrum in MeOH showed absorption bands at λ_{max} 215and 282 nm, while the IR spectrum showed strong absorption bands at 3387 (OH), 1620 (C=C) and 1165 (C-O, 2° alcohol) cm^{-1}.

The ^1H, ^{13}C, and DEPT-135 NMR spectroscopy (Table 1) in combination with 2D ^1H-^{13}C heteronuclear single quantum correlation (HSQC) analysis of (**1**) in DMSO-d_6 (supplementary data, S2–S7) revealed the presence of one *sp3* methylene group H-4′ [δ_H 2.64 (1H, dd, J = 5.0, 16.1 Hz) and δ_H 2.44 (1H, dd, J = 7.0, 16.1 Hz); δ_C 27.9]; one *sp3* methine H-4 [δ_H 4.49 (1H, d, J = 2.0 Hz); δ_C 30.8]; four oxygen-bearing *sp3* methines H-2 [δ_H 5.21 (1H, brs); δ_C 79.9], H-3 [δ_H 4.35 (1H, m); δ_C 70.7], H-2′ [δ_H 4.43 (1H, d, J = 7.1 Hz); δ_C 80.5], and H-3′ [δ_H 3.74 (1H, m); δ_C 66.4]; ten *sp2* aromatic methines grouped by the ^1H-^1H COSY experiment into four spin systems of one 1,2,3-trisubstituted aromatic spin

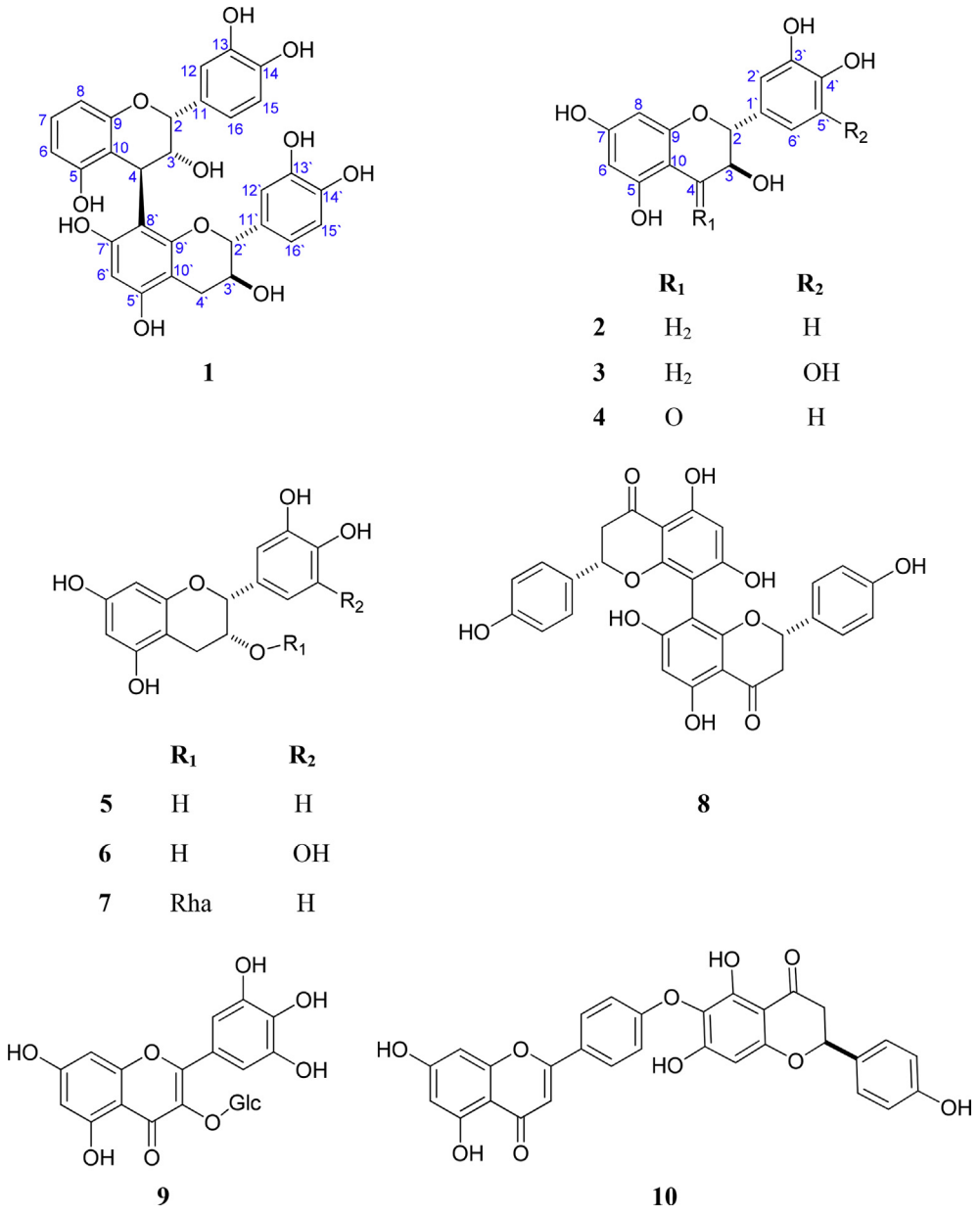

Fig. 1 – Chemical structures of the isolated compounds (1–10); Glc: glucose, Rha: rhamnose.

system H-6 [δ_H 6.15 (1H, d, J = 8.0 Hz), δ_C 107.8], H-7 [δ_H 6.34 (1H, m), δ_C 128.8], and H-8 [δ_H 6.33 (1H, d, J = 8.0 Hz), δ_C 102.3] of ring A upper unit; an isolated aromatic proton H-6′ [δ_H 5.91 (1H, s), δ_C 97.0] of ring A lower unit; and two ABX aromatic systems of H-12 [δ_H 6.69 (1H, s), δ_C 113.0], H-15 [δ_H 6.50 (1H, d, J = 8.0 Hz), δ_C 115.7], and H-16 [δ_H 6.48 (1H, d, J = 8.0 Hz), δ_C 115.8] of ring B upper unit; and H-12′ [δ_H 6.64 (1H, s), δ_C 114.4], H-15′ [δ_H 6.71 (1H, d, J = 8.0 Hz), δ_C 115.5], and H-16′ [δ_H 6.28 (1H, d, J = 8.0 Hz), δ_C 116.9] of ring B lower unit. In addition, 14 quaternary carbon atoms comprising nine oxygenated aromatic carbons C-5, C-9, C-13, and C-14 (δ_C 156.6, 153.9, 145.1, and 144.5 ppm, respectively) of the upper unit and C-5′, C-7′, C-9′, C-13′, and C-14′ (δ_C 155.1, 155.3, 153.6, 144.5, and 144.4 ppm, respectively) of the lower unit; and five non-oxygenated aromatic carbons C-10, C-11, C-8′, C-10′, and C-11′ (δ_C 112.7, 130.9, 104.4, 99.5, and 130.4 ppm, respectively) were observed. Nine hydrogen resonances lacked correlations in the HSQC spectrum of **1** and were therefore recognized as being located on hetero-atoms that were identified subsequently as hydroxyl protons for OH-3 [δ_H 6.84 (1H, brs)] and OH-3′ [δ_H 4.92 (1H, d, J = 4.2 Hz)], in addition to seven hydroxyls on aromatic systems OH-5, OH-13, OH-14, OH-5′, OH-7′, OH-13′, and OH-14′ [δ_H (8.63–9.24)].

The NMR data indicated the structure of dimeric proanthocyanidins with two flavan-3-ol moieties. The presence of two flavanyl units was determined from the ^{1}H and ^{13}C NMR data, with the occurrence of two sets of distinct key signals C-2, C-3, and C-4 for the upper unit, and C-2′, C-3′, and C-4′ for the lower unit [30,31]. The resonance changes of sets indicated that conformational isomerism may exist, which caused by the steric interaction (restricted rotation) between the upper and lower units. This kind of isomerism is well known and observable in many cases of procyanidin oligomers.

Table 1 – ^{1}H (700 MHz) and ^{13}C NMR (175 MHz) data (in DMSO-d_6) for compound 1.

no.	7	
	δ_C, mult.	δ_H, mult (*J* in Hz)
Upper Unit		
2	79.9, CH	5.21, brs
3	70.7, CH	4.35, m
4	30.8, CH	4.49, d (2.0)
5	156.6, C	
6	107.8, CH	6.15, d (8.0)
7	128.8, CH	6.34, m
8	102.3, CH	6.33, d (8.0)
9	153.9, C	
10	112.7, C	
11	130.9, C	
12	113.0, CH	6.69, s
13	145.1, C	
14	144.5, C	
15	115.7, CH	6.50, d (8.0)
16	115.8, CH	6.48, d (8.0)
OH-3		6.84, brs
OH-5		8.63–9.24, s
OH-13		8.63–9.24, s
OH-14		8.63–9.24, s
Lower Unit		
2′	80.5, CH	4.43, d (7.1)
3′	66.4, CH	3.74, m
4′	27.9, CH_2	**a**. 2.64, dd (5.0, 16.1)
		b. 2.44 dd (7.0, 16.1)
5′	155.1, C	
6′	97.0, CH	5.91, s
7′	155.3, C	
8′	104.4, C	
9′	153.6, C	
10′	99.5, C	
11′	130.4, C	
12′	114.4, CH	6.64, s
13′	144.5, C	
14′	144.4, C	
15′	115.5, CH	6.71, d (8.0)
16′	116.9, CH	6.28, d (8.0)
OH-3′		4.92, d (4.2)
OH-5′		8.63–9.24, s
OH-7′		8.63–9.24, s
OH-13		8.63–9.24, s
OH-14		8.63–9.24, s

An analysis of the vicinal coupling constants of the C-ring protons H-2 and H-3 revealed the nature of the units. A large value (7.1 Hz) for $J_{2,3}$ indicated a (+)-catechin unit (2,3-*trans*) for the lower unit and a broad singlet indicated an (−)-epicatechin unit (2,3-*cis*) or epicatechin derivatives (3,5,13,14-flavantetrol unit) [31]. Thus, the upper unit was identified as 3,5,13,14-flavantetrol, whereas the lower unit was identified as (+)-catechin.

The ^{1}H-^{13}C heteronuclear multiple bond correlation (HMBC) analysis of **1** (Fig. 2A) showed the connectivity of the unit based on the observed correlation between H-4 and C-3, C-9, and C-8′, indicating that the connection between the upper and lower units was established between C-4 and C-8′. Comparison of **1** with compounds **2** and **5** showed that dimerization at C-8′ led to a loss of proton H-8′ and a downfield shift of C-8′ from δ_C 94.5 in (**2**) to δ_C 104.4 in (**1**). Moreover, downfield shifts were also observed for C-4 from δ_C 28.3 in (**5**) to δ_C 30.8 in (**1**), for C-3 from δ_C 65.0 in (**5**) to δ_C 70.7 in (**1**), and for C-2 from δ_C 78.1 in (**5**) to δ_C 79.9 in (**1**). Furthermore, key HMBC correlations from H-7 (δ_H 6.34) to C-5 (δ_C 156.6) accompanied by the ^{1}H-^{1}H COSY correlation between H-7/H-6, and H-7/H-8 indicated the loss of the hydroxyl group at C-7 and confirmed the 3,5,13,14-flavantetrol unit.

The absolute configuration at the chiral centre C4, and thus the interflavanoid linkage, was determined from CD spectroscopic data and suggested to be β-configuration (4*R*) owing to a positive Cotton effect at 220–240 nm (Fig. 2B) [31,32]. The systematic conformational analysis was performed by the MOE software package with the Merck Molecular Force Field MMFF94 [33]. The electronic circular dichroism (ECD) was determined for the stable conformers obtained and the geometry was optimized at the B3LYP/6-31G(d) level using the Gaussian09 program package [34]. The overall ECD spectra were then generated according to the Boltzmann weighting of each conformer. Comparison of the theoretical spectra with the experimental spectra revealed a good agreement between the calculated β-configuration (4*R*) and the measured ECD curves (Fig. 2B), whereas the diastereomer α-configuration (4*S*) showed the opposite results. Thus, based on the above evidence, compound **1** was determined to be 3,5,13,14-flavantetrol-(4$\beta\rightarrow$8)-catechin and named rhuspartin.

3.2. *Cytotoxicity assay*

Although compounds **5**, **8**–**10** showed high toxicity toward HUVECs, compounds **1** and **7** were non-toxic even at the highest dose (50 μg/ml). The determined 50% cytotoxicity concentration (CC_{50}) values of the tested compounds (in order) were **5** (2.75 μg/ml), **10** (8.52 μg/ml), **8** (16.47 μg/ml), **9** (18.35 μg/ml), **1** (215.65 μg/ml) and **7** (235.25 μg/ml).

3.3. *Anti-apoptotic or cytoprotective potential of compounds 1 and 7*

The MTT assay showed the dose-dependent anti-apoptotic/cytoprotective activities of compound **1** (Fig. 3A) and compound **7** (Fig. 3B) against MGO-induced apoptosis in HUVECs. Among the four doses tested, the best activity was observed with the highest dose (25 μg/ml) for **7** (approximately 64%) and **1** (approximately 62%), nearing that of the AG (0.05 mM) -treated cells that exhibited approximately 71% reversal of cell apoptosis in relation to MGO toxicity. Tested safe doses above 25 μg/ml did not show significant enhancement in their activities (data not shown).

3.4. *Apoptotic signaling (caspase-3/7) assay*

Further insight into the possible mechanism of HUVEC cytoprotecting or anti-apoptotic activity of compounds **1** and **7** (optimal dose 25 μg/ml) was revealed through downregulation of cellular caspase-3/7 by about 41% and 38%, respectively

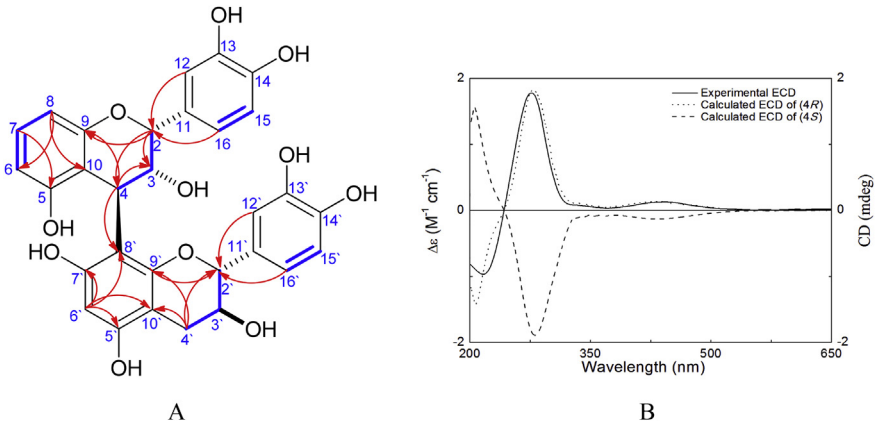

Fig. 2 – A) Selected COSY (▬) and HMBC (H→C) correlations for compound 1. B) Attribution of the absolute configuration of compound (1) by comparing calculated CD spectra with experimental spectra.

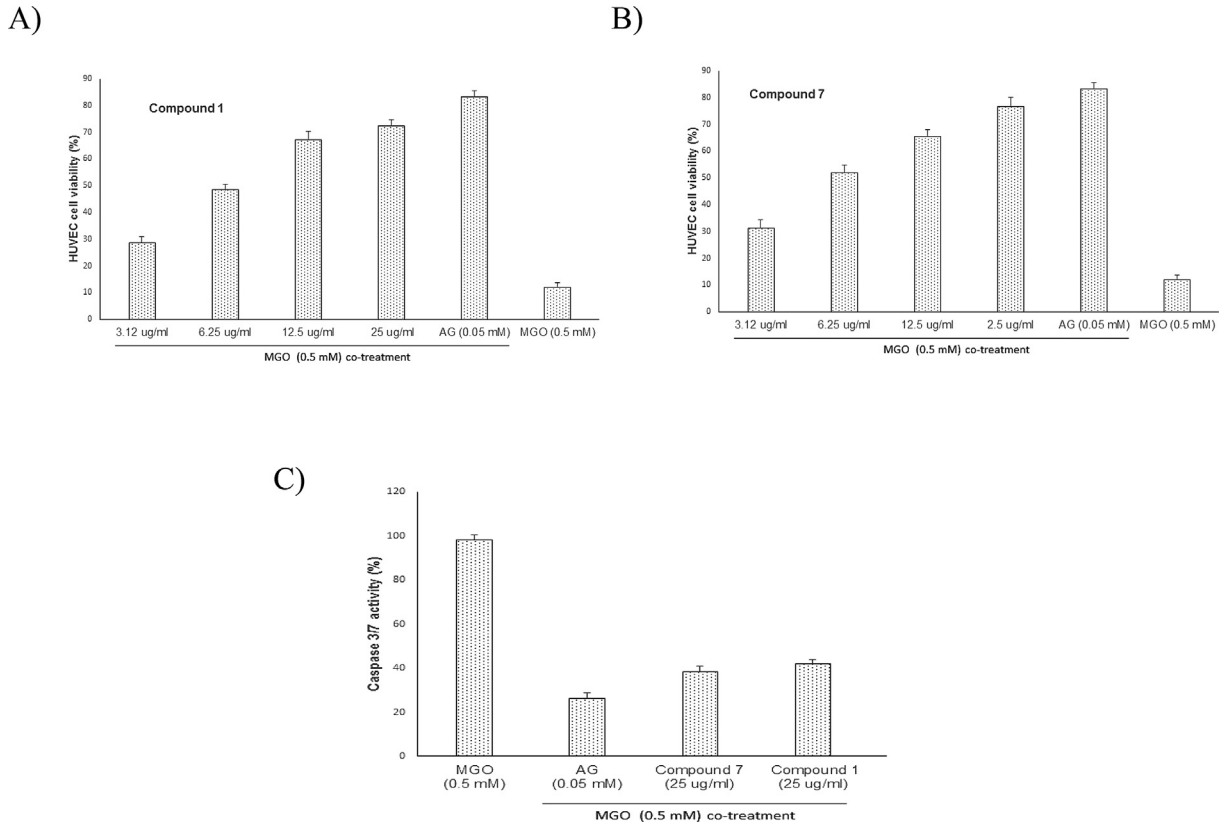

Fig. 3 – MTT assay showing the dose-dependent anti-apoptotic/cytoprotective activity of *R. tripartita* derived compounds 1 (A) and 7 (B) against MGO-toxicity in cultured HUVEC cells. (C) Apoptosis assay showing inhibition of MGO-induced cellular caspase-3/7 activation by *R. tripartita* derived compounds 1 and 7 in cultured HUVEC cells.

compared to AG (approximately 26%) in relation to MGO alone treated cells (Fig. 3C).

This is consistent with the multiple known mechanisms that mediate the damaging effect of MGO on the cells including oxidative stress and disruption of the functionality of cellular proteins, which has negative impact on cell signaling [35]. Similar therapeutic effects have been considered to underlie the effectiveness of a number of chemical compounds which previously shown to protect endothelial cells against carbonyl stress-induced cellular impairments through both antioxidative mechanisms and the modulation of apoptotic gene expression [36].

4. Conclusions

Ten flavonoids, including a new proanthocyanidin (**1**), were isolated and identified from *R. tripartita* stem bark. The

structural determination was performed using extensive NMR and HRESIMS analysis. Of the isolated compounds evaluated for anti-apoptotic effects on cultured HUVECs, the new compound **1** as well as **7** showed cytoprotective potential that reversed the MGO-induced apoptosis through downregulation of caspase3/7.

These data contribute toward the exploration of the structural diversity and biological activity of flavonoids for the prevention and treatment of diabetic cardiovascular diseases. Furthermore, the identified new compound represents a potentially valuable addition to the growing number of proanthocyanidins being isolated from the genus *Rhus*.

Conflicts of interest

All authors declare no conflict of interest.

Acknowledgement

The authors extend their appreciation to the Deanship of Scientific Research at King Saud University for funding this work through the Research Project No R6-17-02-14.

List of abbreviations

AG	aminoguanidine
DMSO-d_6	deuterated dimethylsulfoxide
DPPH	1,1-diphenyl-2-picrylhydrazyl
ECs	endothelial cells
ECD	electronic circular dichroism
HMBC	heteronuclear multiple bond correlation
HRESIMS	high-resolution electrospray ionization mass spectrometry
HSQC	heteronuclear single quantum correlation
HUVEC	human umbilical vein endothelial cells
MGO	methylglyoxal
MTT	MTT3-[4,5-dimethylthiazole-2-yl]-2,5-diphenyltetrazolium) bromide
NMR	nuclear magnetic resonance
TLC	thin-layer chromatography

Appendix A. Supplementary data

Supplementary data to this article can be found online at https://doi.org/10.1016/j.jfda.2019.02.002.

REFERENCES

[1] Tackholm V. In student flora of Egypt. Egypt: Cairo University Press; 1974.
[2] Parveena M, Basudan OA, Mushfiq M, Ghalib RM. A new benzofuranic acid from the leaves of *Rhus alata*. Nat Prod Res 2008;22:371–82.
[3] Kossah R, Nsabimana C, Zhao J, Chen H, Tian F, Zhang H, et al. Comparative study on the chemical composition of Syrian sumac (*Rhus coriaria* L.) and Chinese sumac (*Rhus typhina* L.) fruits. Pak J Nutr 2009;8:1570–4.
[4] Mossa JS, Rafatullah S, Galal AM, Al-Yahya MA. Pharmacological studies of *Rhus retinorrhaea*. Int J Pharmacog 1995;33:242–6.
[5] Shahat AA, Alsaid MS, Rafatullah S, Al-Sohaibani MO, Parvez MK, Al-Dosari MS, et al. Treatment with *Rhus tripartita* extract curtails isoproterenol-elicited cardiotoxicity and oxidative stress in rats. BMC Complement Altern Med 2016;16:351–61.
[6] Alimi H, Mbarki S, Barka ZB, Feriani A, Bouoni Z, Hfaeidh N, et al. Phytochemical, antioxidant and protective effect of *Rhus tripartitum* root bark extract against ethanol-induced ulcer in rats. Gen Physiol Biophys 2013;32:115–27.
[7] Mohammed AE-SI. Phytoconstituents and the study of antioxidant, antimalarial and antimicrobial activities of *Rhus tripartita* growing in Egypt. J Pharmacogn Phytochem 2015;4:276–81.
[8] Shahat AA, Ibrahim AY, Al-Ghamdi AA, Alsaid MS. Phytochemical investigation of *Rhus tripartita* and its activity against cyclooxygenases and acetylcholinesterase. Trop J Pharm Res 2016;15:1697–706.
[9] Mahjoub M, Ammar S, Mighri Z. Isolation and structure studies of a few natural compounds from the Tunisian plant *Rhus tripartitum*. J Soc Alger Chim 2004;14:293–7.
[10] Mahjoub MA, Ammar S, Mighri Z. A new biflavonoid and an isobiflavonoid from *Rhus tripartitum*. Nat Prod Res 2005;19:723–9.
[11] El-Mokasabi F. The state of the art of traditional herbal medicine in the eastern mediterranean coastal region of Libya. Middle East J Sci Res 2014;21:575–82.
[12] Itidel C, Chokri M, Mohamed B, Yosr Z. Antioxidant activity, total phenolic and flavonoid content variation among Tunisian natural populations of *Rhus tripartita* (Ucria) Grande and Rhus pentaphylla Desf. Ind Crops Prod 2013;51:171–7.
[13] Rabbani N, Thornalley PJ. Dicarbonyl proteome and genome damage in metabolic and vascular disease. Biochem Soc Trans 2014;42:425–32.
[14] Nemet I, Varga-Defterdarović L, Turk Z. Methylglyoxal in food and living organisms. Mol Nutr Food Res 2006;50:1105–17.
[15] Lu J, Randell E, Han Y, Adeli K, Krahn J, Meng QH. Increased plasma methylglyoxal level, inflammation, and vascular endothelial dysfunction in diabetic nephropathy. Clin Biochem 2011;44:307–11.
[16] Sena CM, Matafome P, Crisóstomo J, Rodrigues L, Fernandes R, Pereira P, et al. Methylglyoxal promotes oxidative stress and endothelial dysfunction. Pharmacol Res 2012;65:497–506.
[17] Shinohara M, Thornalley P, Giardino I, Beisswenger P, Thorpe SR, Onorato J, et al. Overexpression of glyoxalase-I in bovine endothelial cells inhibits intracellular advanced glycation endproduct formation and prevents hyperglycemia-induced increases in macromolecular endocytosis. J Clin Invest 1998;101:1142–7.
[18] Bourajjaj M, Stehouwer CD, van Hinsbergh VW, Schalkwijk CG. Role of methylglyoxal adducts in the development of vascular complications in diabetes mellitus. Biochem Soc Trans 2003;31:1400–2.
[19] Choy JC, Granville DJ, Hunt DW, McManus BM. Endothelial cell apoptosis: biochemical characteristics and potential implications for atherosclerosis. J Mol Cell Cardiol 2001;33:1673–90.
[20] Abdel-Mageed WM, Al-Wahaibi LH, Backheet EY, El-Gamal AA, Gouda YG, Basudan OA, et al. New phenolic glycosides with cyclooxygenase inhibition from the roots of *Tecoma mollis*. Phytochem Lett 2017;21:98–103.

[21] Abdel-Mageed WM, Backheet EY, Khalifa AA, Ibraheim ZZ, Ross SA. Antiparasitic antioxidant phenylpropanoids and iridoid glycosides from *Tecoma mollis*. Fitoterapia 2012;83:500–7.
[22] Yuan J, Zhu C, Hong Y, Sun Z, Fang X, Wu B, et al. The role of cPLA2 in Methylglyoxal-induced cell apoptosis of HUVECs. Toxicol Appl Pharmacol 2017;323:44–52.
[23] Xu H-Q, Hao H-P, Zhang X, Pan Y. Morroniside protects cultured human umbilical vein endothelial cells from damage by high ambient glucose. Acta Pharmacol Sin 2004;25:412–5.
[24] Davis AL, Cai Y, Davies AP, Lewis J. ^{1}H and ^{13}C NMR assignments of some green tea polyphenols. Magn Reson Chem 1996;34:887–90.
[25] Sheichenko VI, Sheichenko OP, Anufrieva VV, Tolkachev ON, Dyumaev KM, Sokol'skaya TA. NMR study of the phenolic component composition of plant metabolomes. Pharm Chem J 2016;50:83–9.
[26] Porta A. Flavonoid compounds capable of modifying the dynamic and/or physical state of biological membranes and to stimulate the endogenous synthesis of stress proteins in eukaryotic cells, relative synthesis and their use. 2004. Google Patents US 2004/0266699A1.
[27] Subramanyam RM, Srimannarayana G, Subba RN. Structure of mesuaferrone-A, a new Biflavanone from the stamens of *Mesua Ferrea* Linn. Abstract 344 Chemischer Informationsdienst 1978;9:144.
[28] Lin H-Y, Kuo Y-H, Lin Y-L, Chiang W. Antioxidative effect and active components from leaves of Lotus (*Nelumbo nucifera*). J Agric Food Chem 2009;57:6623–9.
[29] Swamy RC, Kunert O, Schühly W, Bucar F, Ferreira D, Rani VS, et al. Structurally unique biflavonoids from Selaginella chrysocaulos and *Selaginella bryopteris*. Chem Biodivers 2006;3:405–14.
[30] Kolodziej H. ^{1}H NMR spectral studies of procyanidin derivatives: diagnostic ^{1}H NMR parameters applicable to the structural elucidation of oligomeric procyanidins. In: Hemingway RW, Laks PE, editors. Plant polyphenols - synthesis, properties, significance. New York: Plenum Press; 1992. p. 295–319.
[31] Esatbeyoglu T, Jaschok-Kentner B, Wray V, Winterhalter P. Structure elucidation of procyanidin oligomers by low-temperature ^{1}H NMR spectroscopy. J Agric Food Chem 2010;59:62–9.
[32] Kolodziej H. Procyanidins from medicinal birch: bonding patterns and sequence of units in triflavanoids of mixed stereochemistry. Phytochemistry 1989;28:3487–92.
[33] MOE. Chemical computing group Inc. 2009. Available at: www.chemcomp.com.
[34] Frisch MJ, Trucks GW, Schlege HBl, Scuseria GE, RobbM A, Cheeseman JR, et al. Gaussian 09, revision B.01. Wallingford CT: Gaussian, Inc.; 2009.
[35] Kalapos MP. The tandem of free radicals and methylglyoxal. Chem Biol Interact 2008;171:251–71.
[36] Tóth AE, Tóth A, Walter FR, Kiss L, Veszelka S, Ózsvári B, et al. Compounds blocking methylglyoxal-induced protein modification and brain endothelial injury. Arch Med Res 2014;45:753–64.